Control of hematopoietic stem cell quiescence by the E3 ubiquitin ligase Fbw7

Benjamin J. Thompson,[1,2,3] Vladimir Jankovic,[4] Jie Gao,[1,2] Silvia Buonamici,[1,2] Alan Vest,[1,2] Jennifer May Lee,[4] Jiri Zavadil,[1,2] Stephen D. Nimer,[4] and Iannis Aifantis[1,2]

[1]Department of Pathology and [2]NYU Cancer Institute, New York University School of Medicine, New York, NY 10016
[3]Medical Scientist Training Program, University of Chicago, Chicago, IL 60637
[4]Molecular Pharmacology and Chemistry Program, Sloan-Kettering Institute, Memorial Sloan-Kettering Cancer Center, New York, NY 10021

Ubiquitination is a posttranslational mechanism that controls diverse cellular processes. We focus here on the ubiquitin ligase Fbw7, a recently identified hematopoietic tumor suppressor that can target for degradation several important oncogenes, including Notch1, c-Myc, and cyclin E. We have generated conditional Fbw7 knockout animals and inactivated the gene in hematopoietic stem cells (HSCs), progenitors, and their differentiated progeny. Deletion of Fbw7 specifically and rapidly affects hematopoiesis in a cell-autonomous manner. Fbw7$^{-/-}$ HSCs show defective maintenance of quiescence, leading to impaired self-renewal and a severe loss of competitive repopulating capacity. Furthermore, Fbw7$^{-/-}$ progenitors are unable to colonize the thymus, leading to a profound depletion of T cell progenitors. Deletion of Fbw7 in bone marrow (BM) stem cells and progenitors leads to the stabilization of c-Myc, a transcription factor previously implicated in HSC self-renewal. On the other hand, neither Notch1 nor cyclin E is visibly stabilized in the BM of Fbw7-deficient mice. Gene expression studies of Fbw7$^{-/-}$ HSCs and hematopoietic progenitors indicate that Fbw7 regulates, through the regulation of HSC cycle entry, the transcriptional "signature" that is associated with the quiescent, self-renewing HSC phenotype.

CORRESPONDENCE
Iannis Aifantis:
iannis.aifantis@med.nyu.edu

Abbreviations used: DN, double negative; ES, embryonic stem; ETP, early T cell progenitor; HSC, hematopoietic stem cell; LSK, lineage−Sca-1$^+$c-Kit$^+$; LT-HSC; long-term HSC; MP, myeloid progenitor; SCF, Skp1/Cul1/F-box protein; T-ALL, T cell–acute lymphoblastic leukemia.

All mature blood cells arise from primitive progenitor cells in the BM. These rare and specialized cells, called hematopoietic stem cells (HSCs), exist mostly in a quiescent state (1). Cell division of HSCs results in both their progressive proliferation and differentiation into increasingly lineage-restricted mature blood cells, as well as maintenance of a small pool of HSCs that do not differentiate, but rather carry out hematopoiesis throughout the life of an organism (2). Much work has been done to elucidate the nature of the signals that govern the balance between self-renewal and differentiation of HSCs. The BM microenvironment in which these cells reside, called the HSC niche, is thought to nurture this balance by providing the appropriate signals (3, 4), but the identities and precise coordination of these signals have only recently begun to be understood.

As the entire life of an HSC revolves around the decisions of whether or not and when to divide, it is no surprise that several molecules and signaling pathways that could regulate cell cycle have been implicated in HSC biology (5–10). For example, the proto-oncogene c-Myc has been shown to be essential for regulating both HSC self-renewal and differentiation (11). The effects of c-Myc deletion in the BM are alleviated by simultaneous deletion of the cell cycle inhibitor p21 (12), underscoring the requirement for strict cell cycle regulation to ensure proper HSC function. Both p21 and c-Myc are regulated at the transcriptional level by the Rho GTPase Cdc42, and deletion of Cdc42 from hematopoietic cells results in increased and decreased levels of c-Myc and p21, respectively, and allows quiescent HSCs to enter the cell cycle and differentiate (13).

In addition to c-Myc, the Notch pathway has also been suggested to influence HSC function. Notch1 signaling is essential during hematopoiesis for the development of T lymphocytes (14, 15), but studies of its role in HSCs have yielded a mixture of results and interpretations. For example, inhibition of Notch1 signaling in vivo

The online version of this article contains supplemental material.

The Rockefeller University Press $30.00
J. Exp. Med. Vol. 205 No. 6 1395-1408 www.jem.org/cgi/doi/10.1084/jem.20080277

can deplete the HSC compartment, possibly by promoting their differentiation into more mature, lineage-restricted cells (7). Also, Stier et al. (16) suggested that Notch pathway activation increases HSC self-renewal in vivo. On the other hand, several genetic studies questioned the importance of Notch1 signaling at this stage. Initially, deletion of the central Notch effector RBP-J (signal binding protein-J) caused no significant HSC or progenitor-specific phenotypes (17). Similarly, no gross hematopoietic defects were reported when either the Notch ligand Jagged1 or the Notch regulators Numb and Numblike were conditionally deleted (18, 19).

Although it is clear that the expression of numerous cell cycle regulators must be tightly controlled in HSCs to permit both their self-renewal and differentiation, the molecular pathways that provide such control are mostly unclear. Notch1 and c-Myc, as well as other cell cycle regulators like cyclin E and c-Jun, are targeted for proteasomal degradation by the E3 ubiquitin ligase, Fbw7 (20, 21). Fbw7 (also called Fbxw7, hCDC4, Ago, and SEL-10) is an F-box protein that serves as a receptor molecule for the Skp1/Cul1/F-box protein (SCF) ubiquitination complex. Fbw7 binds substrates (e.g., Notch1 and c-Myc) by recognizing a phosphorylated motif (a degron) via its WD40 repeat domain (22). Fbw7 is simultaneously bound via its F-box domain to the adaptor protein Skp1, which in turn is bound to the RING finger protein Rbx1 via the scaffold protein Cul1, which allows recruitment of target proteins for poly ubiquitination by an Rbx1-associated ubiquitin-conjugating enzyme (E2) (23); this marks the target protein for degradation by the 26S proteasome (24).

Our laboratory and others have recently shown that inactivating mutations in Fbw7 contribute to the accumulation of Notch1 and c-Myc in T cell–acute lymphoblastic leukemia (T-ALL) (25–27), and several other studies have established Fbw7 as an important tumor suppressor in various tissues (28, 29). Furthermore, growing evidence suggests that the ubiquitin–proteasome system plays diverse and essential roles in stem cell biology (30). The ability of Fbw7 to antagonize cell cycle progression via the ubiquitin–proteasome system prompted us to study the effects of deleting it from hematopoietic cells. As germline Fbw7 knockout mice die in utero around day E10.5 due to defects in vascular development (31, 32), we have generated a conditional allele to allow tissue-specific inactivation of Fbw7 on expression of Cre recombinase. We report here that loss of Fbw7 function leads to a severe depletion of the HSC pool and HSC self-renewal capacity due to the loss of stem cell quiescence. This functional phenotype coincides with a perturbed expression of critical molecular regulators of cell cycle entry in HSCs and a profound decrease in the expression of gene transcripts associated with the HSC self-renewal phenotype.

RESULTS

Fbw7 expression patterns during early hematopoietic differentiation

To study the pattern of Fbw7 expression during early hematopoiesis, we have initially purified the HSC-containing lineage$^-$Sca-1$^+$c-Kit$^+$ (LSK) fraction as well as more differentiated myeloid progenitors (MPs; lineage$^-$Sca-1$^-$c-Kit$^+$), B cell progenitors (B220$^+$CD43$^+$), and thymic T cell (lineage$^-$CD44$^+$25$^+$) progenitors. As shown in Fig. S1 A (available at http://www.jem.org/cgi/content/full/jem.20080277/DC1), Fbw7 mRNA expression was high at the LSK stage and decreased as the cells differentiated into the myeloid lineage (MP: lineage$^-$c-kit$^+$Sca-1$^-$). B cell progenitors expressed moderate amounts of Fbw7 message, whereas in the thymus, the first T cell–committed progenitors (CD44$^+$25$^+$) expressed high amounts of Fbw7. There was no significant expression difference during CD4$^-$8$^-$ to CD4$^+$8$^+$ transition. However, single positive (CD4 or CD8) T cells appear to express lower levels of Fbw7 message (Fig. S1 B). The levels of Cullin 1, a partner of Fbw7 for the formation of the SCF complex, follow similar—although not identical—expression patterns. Finally, to gain further insight in the putative function of Fbw7 during early hematopoiesis, we have generated PCR primers specific for the three distinct Fbw7 isoforms. We were surprised to see that mouse hematopoietic cells express only the Fbw7α isoform that is exclusively localized in the cell nucleoplasm (Fig. S1 C). These studies suggested a dynamic control of Fbw7 expression at different stages of hematopoietic differentiation.

Generation of a conditional Fbw7 allele (Fbw7$^{f/f}$)

As the early lethality of the Fbw7$^{-/-}$ embryos precludes any study of hematopoietic differentiation, we generated an Fbw7-conditional allele targeting exons 5 and 6, as they encode for the F-box domain that is essential for SCF assembly (Fig. 1 A). We have used standard embryonic stem (ES) cell–targeting techniques and "floxed" these two exons with LoxP sites. We have also inserted an Frt-"floxed" Neo mini-gene that was later deleted (Fig. 1 B) from the germline of the generated chimeric progeny (see Materials and methods). Fbw7$^{f/f\ (NEO-)}$ mice were crossed to the IFN-α (and polyI-polyC)–inducible Mx1-cre transgenic mouse stain (33) to generate a model of inducible Fbw7 deletion (Mx-cre$^+$ Fbw7$^{f/f}$). As shown in Fig. 1 (B and C), three polyI-polyC intraperitoneal injections are sufficient to induce total Fbw7 locus deletion and efficiently silence Fbw7 expression in several lymphoid tissues, including the BM, the thymus, and the spleen. The deletion was also total in the BM LSK fraction (see Fig. 8).

Deletion of Fbw7 severely affects hematopoietic progenitor maintenance in the BM

We focused our initial analysis on the early stages of BM hematopoiesis. As early as 2 wk after the end of the polyI-polyC treatment, there was a significant reduction in the absolute number of total BM cells (Fig. 2 A). We should note here that control littermates were either Mx-cre$^+$ Fbw7$^{wt/wt}$ or Mx-cre$^-$ Fbw7$^{f/f}$ mice and were also polyI-polyC injected. As our goal was to study the potential effects of Fbw7 deletion on HSC homeostasis, we turned our attention to the lineage$^-$ compartment. It was immediately obvious that Fbw7 deletion rapidly (at 2 wk after polyI-polyC) and significantly

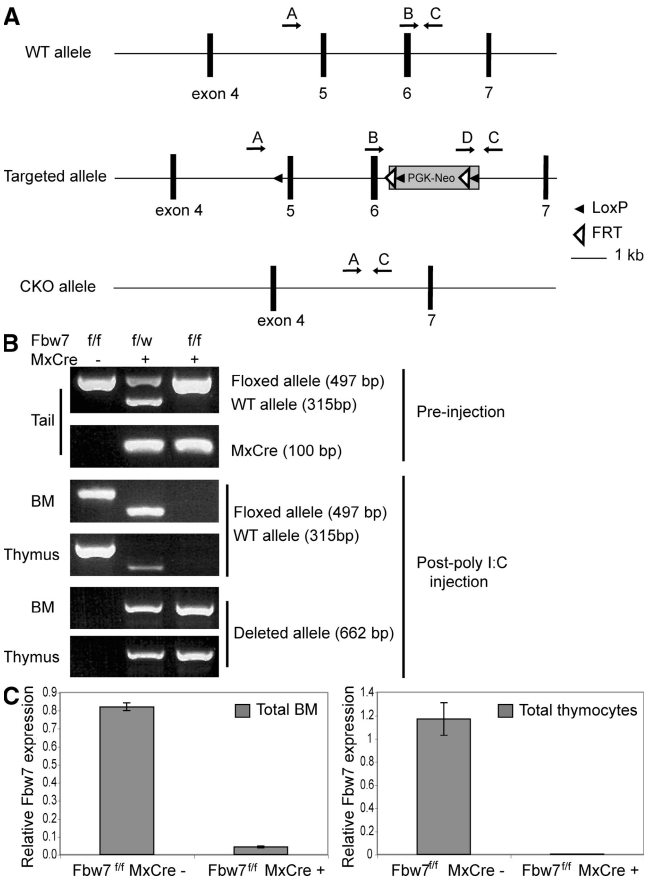

Figure 1. Generation of a conditional Fbw7 allele. (A) Targeting strategy showing exons 4–7 of the mouse genomic Fbw7 locus before targeting (WT allele) and after homologous recombination in C57BL/6 × 129 ES cells (targeted allele), which introduces an FRT- and LoxP-flanked PGK-Neo cassette between exons 6 and 7, and flanks exons 5 and 6 with LoxP sites. Germline removal of the PGK-Neo cassette using the FLPe-deleter strain and subsequent exposure to Cre recombinase results in excision of exons 5 and 6 and generates the conditional knockout (CKO) allele. Arrows show locations of primers (A–D) used to genotype resulting mice. (B) Before crossing to the FLPe-deleter strain, PCR using primers C and D were used to confirm transmission of the targeted allele (not depicted). After removal of the PGK-Neo cassette, primers B and C were used to detect both the "floxed" and WT alleles (497 and 315 bp, respectively). After induction of Mx-Cre with polyI-polyC injections, the floxed band was lost from the BM and thymus, and excision of exons 5 and 6 in these tissues was confirmed by PCR using primers A and C, which amplify 662 bp from the CKO allele. (C) Loss of WT Fbw7 expression was confirmed by quantitative RT-PCR using the same primers as in panel A, which are located in exons 4 and 5. Error bars show the SD of duplicate wells.

affected LSK frequency. Most importantly, absolute numbers of LSK cells decreased three- to fivefold (Fig. 2 B). A significant decrease in the numbers of the first MPs (lineage$^-$ Sca-1$^-$c-Kit$^+$) was also seen, but there were no significant differences in the relative abundance of common, megakaryocyte-erythrocyte, and granulocyte-monocyte progenitors (Fig. 2 E). In agreement with these findings, the LSK frequency in the peripheral blood (not depicted) and spleen (Fig. 2 C) was also decreased. Further subdivision of the LSK fraction to long-term HSC (LT-HSC), short-term HSC, and multipotential progenitors (using a combination of CD34 and c-kit staining) did not reveal any subset-specific effects but suggested a more general effect on LSK homeostasis (Fig. 2 D). As a consequence of the HSC defect, absolute numbers of all BM-mature lineages, including the numbers of immature (B220$^+$IgM$^+$) and mature B cells, were also significantly decreased (Fig. 2 F). These findings strongly suggested that Fbw7 deletion could affect LSK cell self-renewal and/or differentiation in the BM.

Deletion of Fbw7 severely affects progenitor maintenance in the thymus

As LSKs have been shown to represent the major thymus-colonizing population, we analyzed the thymus after Fbw7 deletion and found no significant change in total thymocyte numbers 2 wk after polyI-polyC deletion (Fig. 3 A). However, at later time points (4 wk after polyI-polyC) Mx-cre$^+$ Fbw7$^{f/f}$ thymocyte numbers were significantly decreased (Fig. 3 A). Notch1 appeared to be the main Fbw7 substrate in the thymus, as its deletion led to a significant accumulation of intracellular Notch1 protein as detected by two different Notch1-specific antibodies (Fig. S2 A, available at http://www.jem.org/cgi/content/full/jem.20080277/DC1). This finding was consistent with our recent identification of Notch1 as a substrate of Fbw7 in T cells. Supporting this observation, Deltex1 transcription, a reliable Notch1 reporter, was significantly up-regulated in Mx-cre$^+$ Fbw7$^{f/f}$ thymi (Fig. S2 B). On the other hand, other putative Fbw7 substrates like c-Myc or cyclin E were not significantly stabilized in total Mx-cre$^+$ Fbw7$^{f/f}$ thymocytes at this specific time point (Fig. S2 A).

As evident from Fig. 3 B, Fbw7 deletion appeared to significantly affect the most immature (CD4$^-$8$^-$) thymocytes as both their frequency and their absolute numbers decreased two- to sixfold (Fig. 3, B and C). As this CD4$^-$8$^-$ double negative (DN) population includes the most immature T cell progenitors, we have further subdivided this subset using antibodies against CD25, CD44, and c-kit. This analysis revealed an almost complete absence of both DN2 (CD25$^+$44$^+$) and DN3 CD44$^-$25$^+$ thymocytes (Fig. 3, D and E). These phenotypes depended on the timing of the deletion mediated by the Mx1 promoter that is active both in thymocytes and their immediate BM progenitors. Indeed, when we deleted Fbw7 only in developing thymocytes using the Lck promoter (34) (Lck-cre$^+$Fbw7$^{f/f}$), none of these DN cell–specific phenotypes were obvious (Fig. 3 F and Fig. S3 A). This could be explained by the later Fbw7 gene deletion in the Lck-cre model (Fig. S3 B). 4-wk-old Lck-cre$^+$Fbw7$^{f/f}$ mice had thymocyte numbers similar to Lck-cre$^+$Fbw7$^{wt/wt}$ control littermates, and almost 50% of them developed T cell lymphomas later in life (unpublished data and reference 35). Both Notch1 and c-Myc appeared to be stabilized in the thymi of these mice. Notch1 was also stabilized in immature CD4$^-$8$^-$ thymocytes (not depicted). To further investigate the hypothesis that the thymic phenotype was at least partially due to the decreased number

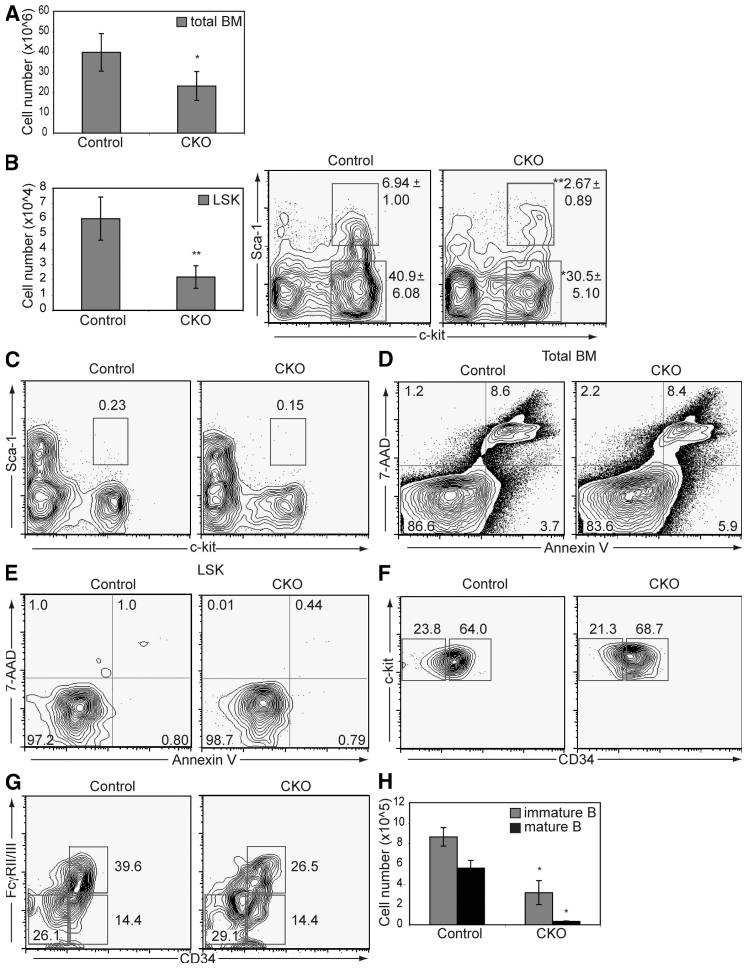

Figure 2. Fbw7 deletion leads to a depletion of BM hematopoietic progenitors. (A) Absolute numbers of BM cells in polyI-polyC–injected control (Fbw7$^{f/f}$, MxCre^{-}) and CKO (Fbw7$^{f/f}$, MxCre^{+}) mice 2 wk after polyI-polyC deletion are shown. (B) Lin^{-} BM cells were stained for c-kit and Sca-1 to mark the LSK population (dot plot), and absolute LSK numbers (histogram) were calculated (also at 2 wk after polyI-polyC). (C) Quantitation of peripheral (spleen) LSKs 2 wk after polyI-polyC injection. $P < 0.05$. (D and E) Absence of enhanced rates of apoptosis as defined by a combination of 7-AAD/annexin V staining in either total BM of LSK cells (3 wk after polyI-polyC injection). (F) LSK cells were analyzed by FACS for CD34 expression to separate long-term (LT, CD34^{-}) from short-term (ST, CD34^{+}) HSCs. (G) MPs (Lin^{-}/Sca-1^{-}/c-kit^{+}) were analyzed by FACS for CD34 and FcγRII/III expression to show common MPs (CMP, CD34^{+}/ FcγRII/III^{-}; bottom right gate), granulocyte/macrophage progenitors (GMP, CD34^{+}/ FcγRII/III^{+}; top right gate), and megakaryocyte/erythroid progenitors (MEP, CD34^{lo} / FcγRII/III^{-}; bottom left gate). (H) Absolute number of mature (IgM^{+}/B220^{hi}) and immature (IgM^{+}/B220^{+}) BM B cells are shown (2 wk after polyI-polyC). Error bars show the SD. Numbers indicate the percentage of cells in each gate. *, $P < 0.05$; **, $P < 0.005$. For all experiments, $n = 8$.

of entering BM stem and progenitor cells, we have quantified the absolute number of the first thymic immigrants (early T cell progenitors [ETPs], defined as lineage^{-}CD25^{-}c-kit^{high} cells) in the thymi of control and mutant mice 2 and 4 wk after polyI-polyC injection. As shown in Fig. 3 G, ETP numbers were significantly decreased upon Fbw7 deletion at both time points. Our studies demonstrated that deletion of Fbw7 using the Mx-cre^{+}Fbw7$^{f/f}$ model severely affects lymphocyte development in the thymus.

Loss of Fbw7 leads to a cell-autonomous defect of stem cell self-renewal

As the Mx1 promoter is IFN-α responsive and can drive cre-recombinase expression in nonhematopoietic lineages (e.g., the BM HSC niche), we have tested whether the reported phenotypes were cell autonomous. We used a competitive transplantation assay mixing Mx-cre^{+}Fbw7$^{f/f}$ or Mx-cre^{+} Fbw7$^{wt/wt}$ CD45.2^{+} BM cells (from polyI-polyC–injected mice) with CD45.1^{+} WT cells. At the time of the injection, we had normalized for absolute numbers of LSK cells and injected ~10^3 LSK cells from each genotype. These cells were transplanted in irradiated CD45.1 hosts, and chimerism was studied 5 wk later. We should note here that in this assay we expected <50% CD45.2 chimerism due to the existence of endogenous, host-derived CD45.1^{+} cells. The exact CD45.2 chimerism depended on the injection efficiency and in our hands varied from 10 to 45%. Indeed, although Mx-cre^{+}Fbw7$^{wt/wt}$ cells efficiently competed (generating >40%

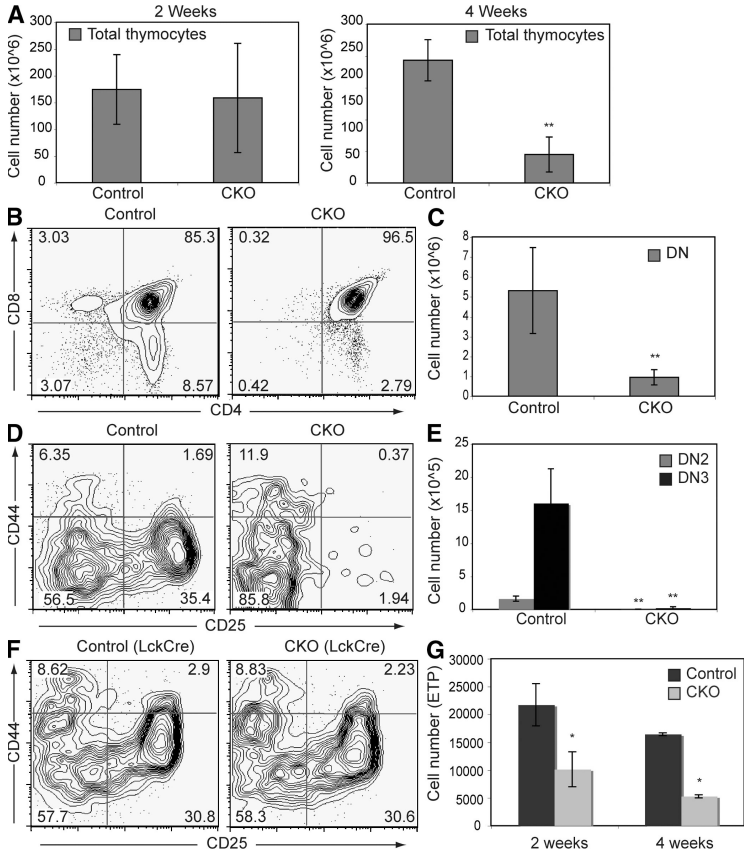

Figure 3. Loss of Fbw7 severely impairs early T cell development. (A) Absolute numbers of thymocytes (left, 2 wk after polyI-polyC; right, 4 wk after polyI-polyC) were counted from control ($n = 8$) and CKO ($n = 8$) mice and analyzed by FACS for CD4 and CD8 expression (B). (C) Absolute numbers of $CD4^-8^-$ DN cells (2 wk after polyI-polyC). (D) DN cells were separated into DN1–4 populations by staining for CD44 and CD25. (E) Absolute numbers of DN2 ($CD44^+/CD25^+$) and DN3 ($CD44^-/CD25^+$) (2 wk after polyI-polyC). (F) DN thymocytes were analyzed as in D in control ($Fbw7^{f/f}$, $LckCre^-$) and CKO ($Fbw7^{f/f}$, $LckCre^+$) mice. Error bars show the SD. Numbers indicate the percentage of cells in each gate. **, $P < 0.005$. $n = 6$. (G) Absolute numbers of ETP ($Lin^-CD25^-CD44^+c\text{-}kit^+$) cells 2 and 4 wk after polyI-polyC injection. *, $P < 0.05$. $n = 4$.

chimerism) with CD45.1 BM, Mx-$cre^+Fbw7^{f/f}$ cells generated only minimal chimerism in the spleen, thymus, and BM of the recipient animals, suggesting a very severe defect in their ability to differentiate and replenish the hematopoietic and immune systems (Fig. 4 A). Interestingly, when we studied chimerism in the LSK compartment we found almost no $Fbw7^{-/-}$ LSK cells (Fig. 4 B). Similarly, in the BM, <3% of total BM mononuclear cells derived from $Fbw7^{-/-}$ progenitors. Very few of these cells managed to properly differentiate toward the myeloid (not depicted) or B cell lineage (Fig. 4 C). Moreover, <0.1% of total donor-derived thymocytes originated from $Fbw7^{-/-}$ BM. Once more, these cells failed to differentiate to the $CD4^+8^+$ stage, and the vast majority belonged to the early $CD44^+25^+$ DN1 stage (Fig. 4, D and E). These experiments demonstrated that $Fbw7^{-/-}$ stem cells were unable to compete with WT counterparts.

As the previous results could also be explained by altered the homing ability of HSCs upon Fbw7 deletion, we altered our transplantation protocol so that we transplanted 0.5×10^6 non-polyI-polyC–injected (Mx-$cre^+Fbw7^{f/f}$ or Mx-$cre^+Fbw7^{wt/wt}$) $CD45.2^+$ BM cells with an equal number of $CD45.1^+$ WT cells into irradiated CD45.1 hosts and documented chimerism 3 wk later. Only after transplant did we inject the recipients with polyI-polyC (three times) to delete the Fbw7 locus. 7 wk after polyI-polyC injection, we found no (or very few) mature donor-derived $Fbw7^{-/-}$ cells (thymocytes, B cells, $Mac1^+$, $NK1.1^+$, and $Gr\text{-}1^+$ cells), including BM LSK (Fig. S4, available at http://www.jem.org/cgi/content/full/jem.20080277/DC1). These combined transplantation results strongly demonstrated that the Fbw7 deletion-induced phenotype is cell autonomous and is not due to the inability of Fbw7 LSK to home to the marrow niche.

Deletion of Fbw7 leads to defective HSC quiescence and self-renewal

To begin understanding the molecular mechanism behind the HSC defect caused by the deletion of Fbw7, we initially studied LSK survival in the BM of polyI-polyC–injected animals (at 2, 3, and 4 wk after injection). No significant differences in the percentage of apoptotic LSK in polyI-polyC–injected littermate mice (Mx-$cre^+Fbw7^{f/f}$, Mx-$cre^+Fbw7^{wt/wt}$, or Mx-$cre^+Fbw7^{f/w}$) were observed at 3 wk after polyI-polyC (Fig. 2),

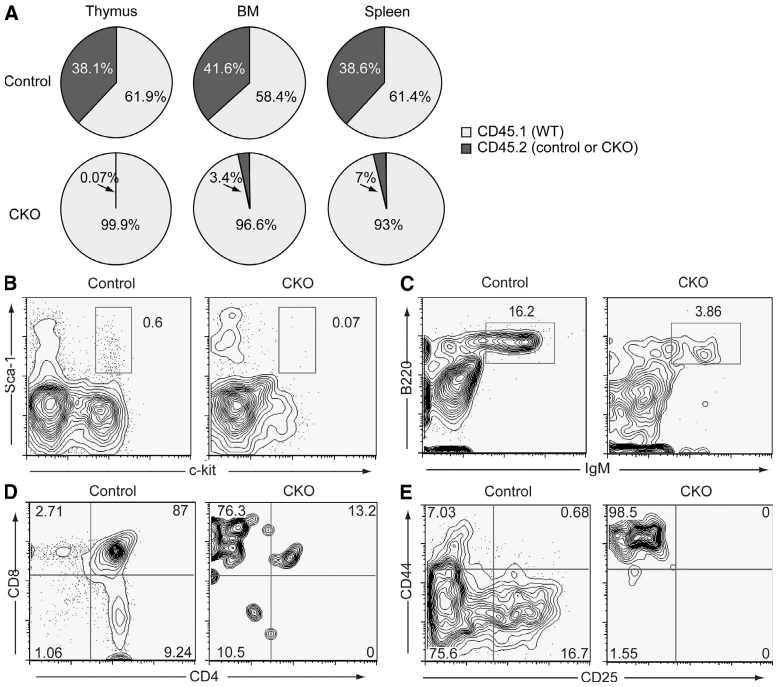

Figure 4. Loss of Fbw7 leads to a cell-autonomous defect of HSC self-renewal. (A) 0.5×10^6 WT CD45.1 BM cells were injected into lethally irradiated WT Ly 5.1^+ host mice ($n = 3$ for each experiment) with the same number of either control CD45.2 or CKO (Mx1-cre$^+$Fbw7$^{f/f}$) CD45.2 BM cells. The mice were analyzed 5 wk later for reconstitution of the BM, thymus, and spleen by staining cells from each tissue for both CD45.1 and CD45.2. The percent contribution of each donor to those organs is shown. CD45.2-gated cells from recipient mice were analyzed by FACS for expression of CD4, CD8, CD44, and CD25 in the thymus (D and E), B220/IgM (C), and LSK markers (B) in the BM. The cells in E are gated on the thymic Lin$^-$ population. Numbers indicate the percentage of cells in each gate.

arguing against the involvement of the SCF^{Fbw7} complex in LSK survival.

To address the effect of Fbw7 deletion on stem cell proliferation, we used Ki67 and DAPI labeling to determine the cell cycle status of LSK cells. The percentage of Mx-cre$^+$Fbw7$^{f/f}$ LSK cells that passed the G0-G1 checkpoint and entered cycle was consistently and significantly elevated when compared with Mx-cre$^+$Fbw7$^{wt/wt}$ counterparts (Fig. 5 A). Interestingly, these effects appear to be LSK specific, as more differentiated cell populations (MPs, T cell progenitors, CD4$^+$8$^+$ thymocytes) do not show similar cell cycle acceleration (Fig. S5, available at http://www.jem.org/cgi/content/full/jem.20080277/DC1). To further support these findings, we have used a short (42-h) pulse of BrdU to mark cells that escape quiescence and enter the cell cycle, and subdivided the LSK compartment into CD34$^-$ (self-renewing LT-HSC) and CD34$^+$ (non-self–renewing short-term–HSC and MPP) subsets. As evident from Fig. 5 B, Fbw7$^{-/-}$ LT-HSCs showed a dramatic loss of quiescence, as almost 80% of them entered cell cycle during the 42 h from the initiation of the BrdU pulse. CD34$^+$ LSK cells also showed a significantly elevated fraction of BrdU$^+$ cells. We should also note here that LSK cycle deregulation was evident even in marrows with less significant alterations in LSK or total cell numbers, suggesting that the functional changes preceded the phenotypic ones (not depicted).

We then asked whether this loss of quiescence translates to defective HSC self-renewal or differentiation. We used colony-forming cell assays and initially plated total BM from polyI-polyC–treated Mx-cre$^+$Fbw7$^{wt/wt}$ or Mx-cre$^+$Fbw7$^{f/f}$ animals and incubated them in semi-solid methylcellulose medium in the presence of a suitable cytokine cocktail. As shown in Fig. 5 C, Mx-cre$^+$Fbw7$^{f/f}$ cells generated only half the number of colonies compared with Mx-cre$^+$Fbw7$^{wt/wt}$ progenitors. Also, these colonies were significantly smaller in size (Fig. 5 E). We then performed similar experiments using highly enriched CD34$^-$ LT-HSCs. Interestingly, during the initial plating no differences in the absolute numbers of colonies were recorded. However, the replating of colonies that originated from Mx-cre$^+$Fbw7$^{f/f}$ LT-HSCs showed a complete loss of self-renewal capacity (Fig. 5 D) in agreement with our in vivo competitive reconstitution assays (Fig. 4). These observations clearly showed that Fbw7 deletion promotes aberrant cell cycle entry and loss of self-renewal.

BM Fbw7 deletion leads to c-Myc protein stabilization

As Fbw7 is able to ubiquitinate and degrade several target proteins, we performed an initial protein expression screening of three well-characterized substrates, Notch1, c-Myc, and cyclin E (Fig. 6). We were unable to detect significant expression and stabilization of either Notch1 or cyclin E in total BM cells. This result was not surprising, as Notch1 mRNA is

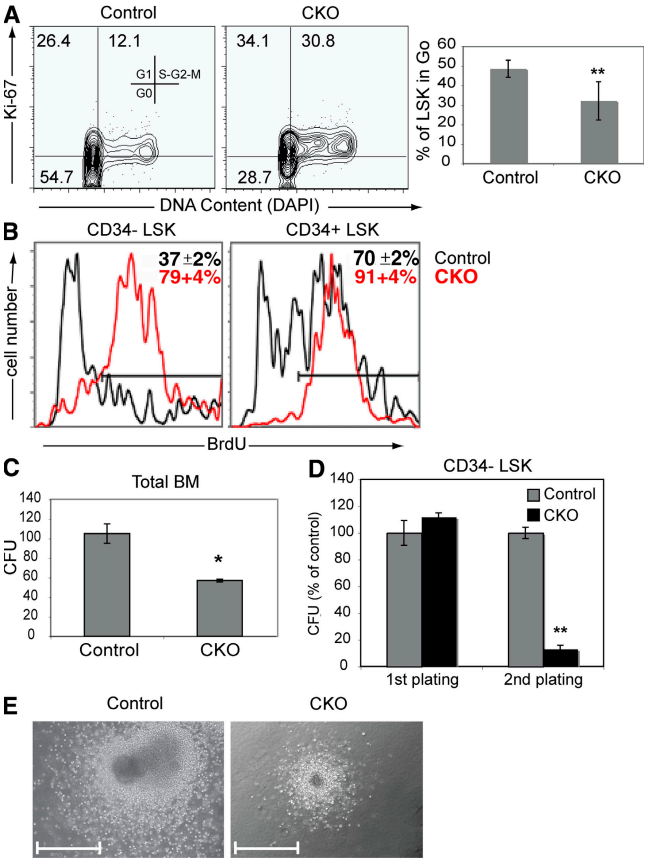

Figure 5. Deletion of Fbw7 leads to defective HSC quiescence and self-renewal. (A) LSK control and Mx1-cre^{+}Fbw7$^{f/f}$ (CKO) mice were further analyzed for DNA content (DAPI) and intracellular Ki-67 expression (2 wk after polyI-polyC). Quadrants correspond to cell cycle stages as shown in the left panel. The percentage of LSK cells in G0 stage is also shown ($n = 6$), (B) BrdU labeling of the CD34^{-} and CD34^{+} LSK subsets ($n = 4$) (2 wk after polyI-polyC). (C) 25,000 total BM cells from control or CKO mice were plated in methylcelluose medium containing a multilineage cytokine cocktail. The number of colonies and their qualitative morphologies were determined 8 d later. (D) The same experiment as in C was performed, except plating 500 flow-purified LT-HSCs per plate. After 7 d, the colonies were counted (first plating). The colonies from each plate were pooled and resuspended in PBS, and 2,000 of those cells were replated for an additional 7 d before counting colonies again (second plating). Numbers indicate the percentage of cells in each gate. (E) Photographs of representative colonies from C (first plating) show the relative size difference between control- and CKO-derived colonies. Bar, 0.5 mm. These are representatives of at least three individual experiments. *, $P < 0.05$; **, $P < 0.005$.

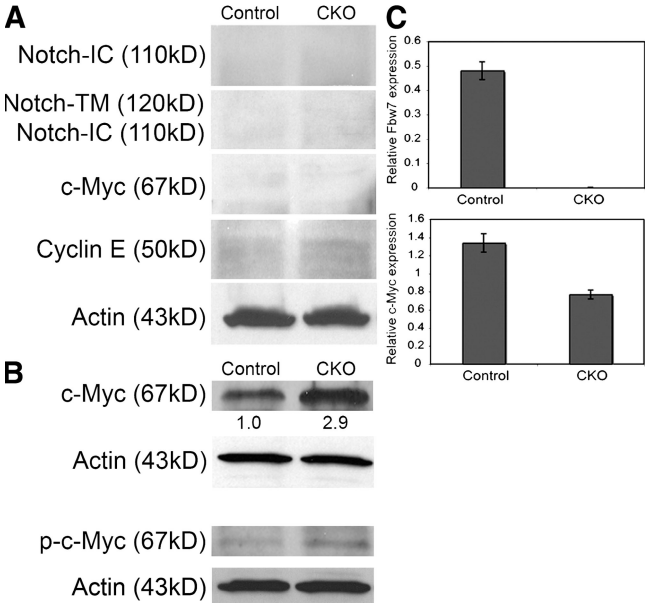

Figure 6. Effects of Fbw7 deletion on target protein stabilization in the BM. (A) Western blot detecting expression of Notch1-IC, uncleaved membrane Notch1 (Notch1-TM), c-Myc, cyclin E, and b-actin in total BM extracts. (B) Expression of c-Myc in cytokine-stimulated BM progenitors. Lineage^{-}IL-7Rα^{-}Sca-1^{high}c-kit^{high} cells from control and CKO (Mx-cre^{+}Fbw7$^{flox/flox}$) mice were cultured for 48 h in the presence of cytokines. c-Myc expression was quantified using densitometry and actin normalization. Phospho–c-Myc (T58/S62) and actin levels are also shown. A representative of three experiments is shown. (C) Quantitative RT-PCR quantifying expression of Fbw7 and c-Myc in the cells used in B. Expression is normalized using b-actin.

not expressed in mature myeloid/erythroid/B cells that comprise the vast majority of the marrow. Also, cyclin E is expressed in a small fraction of actively cycling progenitors (36). Similarly, c-Myc expression was difficult to detect (Fig. 6 A). Once more, this was an anticipated finding, as c-Myc is only expressed in a small fraction of BM cells (unpublished data).

These observations suggested that we should focus our attention on the small fraction of BM cells that includes putative stem cells and progenitors. We have thus sorted LSK cells from polyI-polyC–injected Mx-cre^{+}Fbw7$^{f/f}$ mice (and Mx-cre^{+}Fbw7$^{wt/wt}$ controls). We placed these cells in a liquid culture in the presence of cytokines as shown in Fig. 7. Once more, we have detected no stabilization of either Notch1 or cyclin E (not depicted). On the other hand, c-Myc protein was substantially overexpressed (almost threefold). Also, the accumulated c-Myc protein was phosphorylated on the T58 and S62 residues, in agreement with the idea that phospho species of the c-Myc substrate should accumulate in the absence of proteasomal degradation (Fig. 6 B). Further quantitative RT-PCR experiments have proven that the c-Myc stabilization was due to posttranslational modification (Fig. 6 C). This c-Myc stabilization was persistent between different experiments. These results (Fig. 6 C) suggested that Fbw7 deletion in stem cell and progenitor populations led to a significant stabilization of c-Myc but not Notch1 or cyclin E proteins.

Dynamic regulation of Fbw7 expression during HSC cycle entry and differentiation

Previously presented results suggest that Fbw7 is an HSC cycle entry "brake" and that its deletion affects HSC quiescence. In agreement with this scenario, Fbw7 expression is significantly down-regulated as LSKs differentiate to become

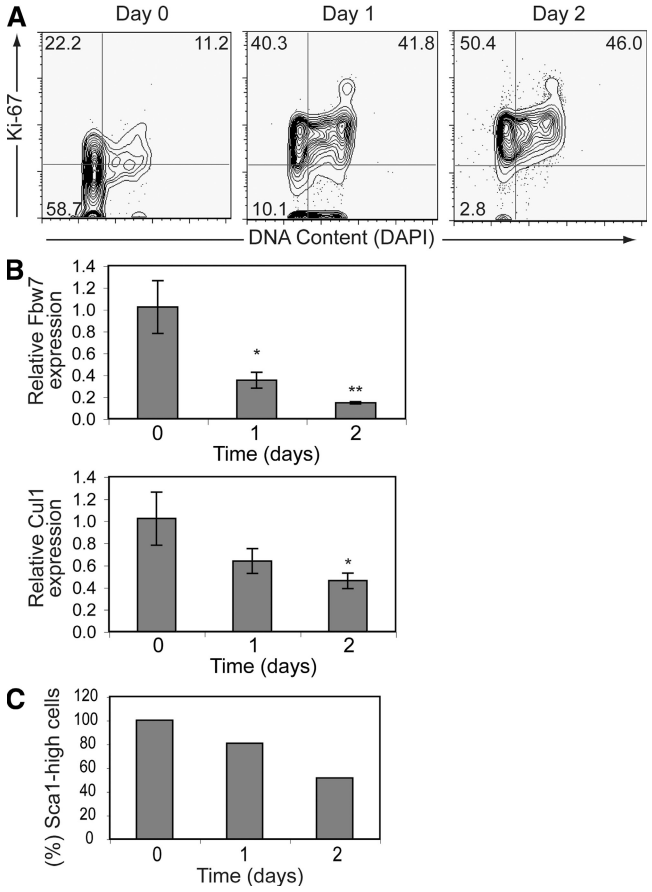

Figure 7. Dynamic regulation of Fbw7 expression during HSC cycle entry and differentiation. (A) Flow-purified LSK cells were cultured with cytokines for 0, 1, or 2 d and were stained for intracellular Ki-67 and DNA content (DAPI). (B) Fbw7 and Cul1 mRNA expression were analyzed by quantitative RT-PCR on each day. (C) Quantification of Sca-1 expression (loss of Sca-1 indicates differentiation of LSK cells) after each day of culture. On day 0, all cells are Sca-1$^+$.

MPs (Fig. S1). To further understand the role of Fbw7 during physiological HSC proliferation and differentiation, we purified LSK cells and placed them in cytokine-driven in vitro cultures. Before the cytokine stimulation (day 0), almost 60% of the cells were in G0. Upon stimulation, cells rapidly entered cycle with only 2–3% of cells in G0 at day 2 (Fig. 7 A). Fbw7 expression declined significantly in response to cytokine stimulation, and Cul1 expression followed an identical pattern (Fig. 7 B). Although these results suggested that Fbw7 expression is dynamically regulated at the HSC stage, it is difficult to uncouple proliferation from differentiation-triggered effects. We further quantified cell differentiation by measuring the proportion of cells that lost Sca-1 expression. As shown in Fig. 7 C, at day 1 almost 80% of the cells retained their c-kit$^+$Sca-1$^+$ phenotype, whereas Fbw7 expression was decreased three- to fourfold. Although effects of differentiation are not excluded, this observation suggested that Fbw7 message expression is down-regulated as HSCs enter cell cycle.

Fbw7 controls a gene program that correlates with HSC quiescence and self-renewal

To further characterize the molecular mechanism of Fbw7 function in the differentiation and homeostasis of HSCs, we have performed a whole transcriptome analysis. We have used FACS-purified lineage$^-$IL7Rα^-c-kit^{high}Sca-1^{high} stem/multilineage progenitors (LSK) and lineage$^-$IL7Rα^-c-kit^{high}Sca-1$^-$ MPs from polyI-polyC–injected pooled Mx-cre$^+$Fbw7$^{f/f}$ and Mx-cre$^+$Fbw7$^{wt/wt}$ littermate mice, extracted total RNA, and used it for microarray analysis. Both the array analysis (not depicted) and quantitative RT-PCR (Fig. 8 A) showed that deletion of the Fbw7 locus and silencing of its expression in the LSK and MP compartments used for these experiments were complete.

We have performed an analysis of genes that showed a greater than or equal to threefold difference in expression between the control and Fbw7$^{-/-}$ LSK cells. This analysis demonstrated that Fbw7$^{-/-}$ LSK cells were more closely related to the differentiated MP populations than the control LSK subset (not depicted). The combination of published studies (37–40) and our own results (Table S1, available at http://www.jem.org/cgi/content/full/jem.20080277/DC1, and unpublished data) suggested a partial transcriptional "signature" associated with the LT-HSC phenotype. These transcripts are enriched in LT-HSCs and down-regulated upon the loss of self-renewal properties. We thus hypothesized that the transcriptional signature of Fbw7 deletion in HSCs contains the features of the physiological loss of stem cell phenotype associated with the commitment to the transiently amplifying progenitor fate. Such a hypothesis was supported by the identities of genes specifically affected by Fbw7 deletion in the LSK compartment (not depicted), including *Evi1*, *Mpl*, *p57*, *Agpt*, *Eya1/2*, *Pbx3*, and *Meis1*, which were all previously shown to be enriched in self-renewing HSCs (Table S1). These results were further verified using quantitative RT-PCR analysis of distinct biological samples (Fig. 8 B) and were perfectly in line with the presented phenotypic results, which suggested a loss of HSC quiescence and self-renewal capacity upon Fbw7 deletion. Importantly, the observed global loss of HSC-specific transcriptional signature was not an artifact from contaminating Sca-1$^{low/-}$ cells, as the Ly6A (Sca-1)–specific signal was even slightly higher in the Fbw7$^{-/-}$ compared with the control LSK sample (not depicted).

This loss of "LT-HSC–specific" gene expression was accompanied by the activation of a more differentiated gene expression program in cells that lose Fbw7 expression. Indeed, several genes suggesting an erythro-myeloid and lymphoid priming (38) were up-regulated upon Fbw7 loss (i.e., glycophorin A, CD36, neutrophil elastase, Rag-1, etc.; not depicted). This is consistent with the presented expression analysis data that show that Fbw7 mRNA expression decreases during the transition of undifferentiated LSK cells to the committed progenitor stage, which could be a functional part of the early HSC differentiation program.

Finally, we have searched for genes that could explain the loss of stem cell quiescence upon Fbw7 deletion. As shown in

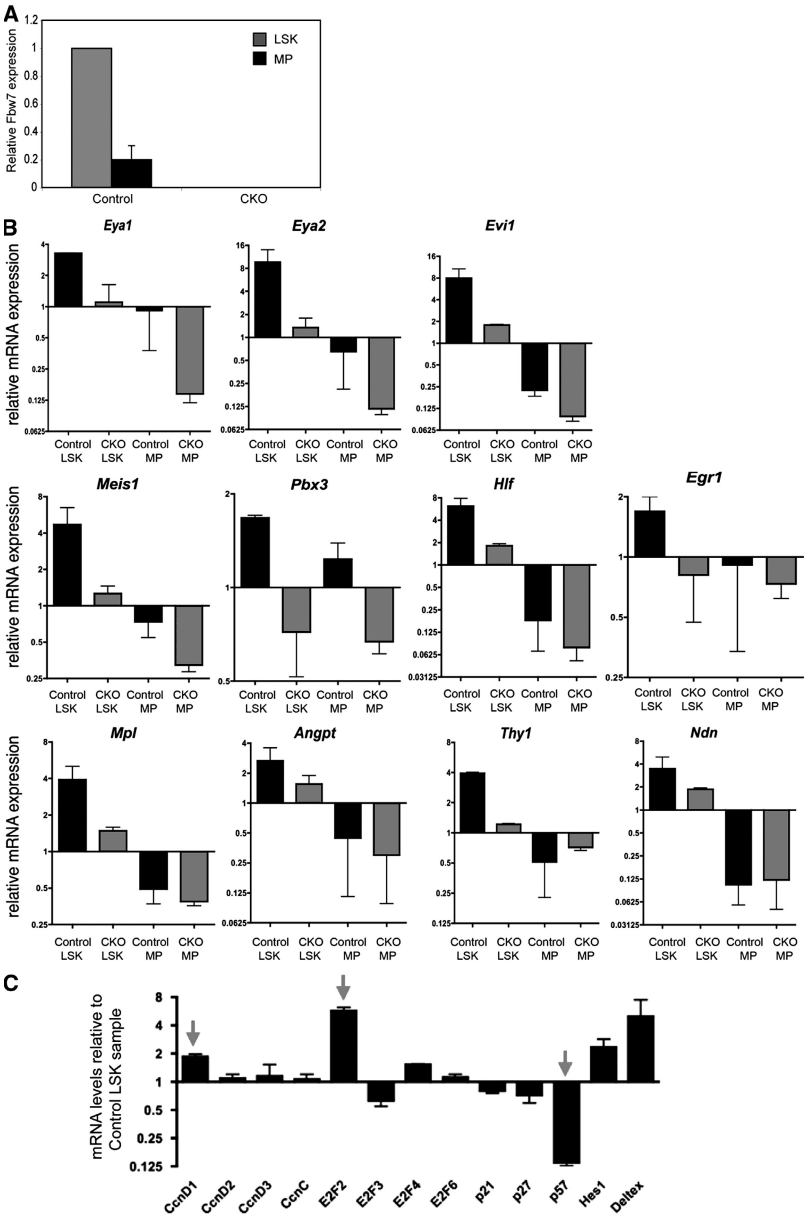

Figure 8. Fbw7 controls genes that correlate with HSC quiescence and self-renewal. (A) Efficient silencing of Fbw7 expression in LSK cells and MPs in response to polyI-polyC treatment (at 2 wk after treatment). (B) Quantitative RT-PCR validation of genes selected from the microarray using mRNA from a different sorting experiment. The plotted expression values represent the relative mRNA level of each sample normalized to the median expression across all samples. (C) Quantitative RT-PCR analysis of the expression of multiple cell cycle–related genes in control (Mx-cre^{+}Fbw7$^{+/+}$) and CKO (Mx-cre^{+}Fbw7$^{fl/fl}$) LSK cells.

Fig. 8 C, several cell cycle regulators, including p27, p21, and Ccnd2/3, were unaffected by the deletion of Fbw7. However, the expression of three cell cycle–related genes was altered in response to Fbw7 silencing. The cyclin kinase inhibitor p57^{kip2}, previously implicated in loss of quiescence of stem cells (38), was down-regulated in Mx-cre^{+}Fbw7$^{f/f}$ LSK cells. On the other hand, the cell cycle regulator E2F2 was significantly up-regulated upon Fbw7 loss. Finally, the D-type cyclin Ccnd1 was up-regulated after Fbw7 gene excision, in agreement with its role in HSC cycle entry. Interestingly, all three genes have been previously suggested to be targets of c-Myc, supporting our view that c-Myc overexpression could be an important regulator of cell cycle entry downstream of Fbw7 (41–43). The presented expression studies provide a very strong mechanistic basis that explains the phenotypic and functional effects of Fbw7 deletion on HSC quiescence and self-renewal.

DISCUSSION

In this report we demonstrate that a single E3 ubiquitin ligase, Fbw7, is an essential regulator of HSC quiescence and

self-renewal. Fbw7 is expressed in quiescent HSCs, and its expression is down-regulated upon the loss of their self-renewing capacity. These effects are cell autonomous, as Fbw7$^{-/-}$ LSKs are unable to compete with WT counterparts both in vitro and in vivo. The loss of LSK absolute numbers and self-renewal abilities are also reflected at the early stages of lymphopoiesis, as Mx-cre^{+}Fbw7$^{f/f}$ mice have lower numbers of B cell, and almost no T cell, progenitors. To mechanistically explain these LSK phenotypes, we have performed comparative gene expression studies using Fbw7$^{-/-}$ stem cells and MPs. These studies demonstrated that Fbw7 deletion targets specific cell cycle regulators and suppresses the expression of several genes previously suggested to control HSC function. Thus, we have identified a novel function for the proteasome–ubiquitin ligase complex as a genetic "switch" that controls HSC cycle entry and self-renewal.

Our studies are in agreement with a recent report by Matsuoka et al. (44). These investigators also demonstrate that Fbw7 is essential to maintain HSC quiescence and self-renewal, and suggest that c-Myc is a key Fbw7 substrate in HSCs. They also report that Fbw7$^{-/-}$ animals die by either extreme pancytopenia at 12 wk after polyI-polyC injection or by T-ALL. Development of T-ALL was a later event, as disease appeared only after 16 wk after treatment. Only very few (n = 2) of our polyI-polyC–injected Fbw7$^{f/f}$ animals were allowed to reach these time points, and all developed pancytopenia. Thus, we cannot directly compare rates of T-ALL induction, as all other polyI-polyC–injected animals presented in this study were analyzed at very early time points. However, both Fbw7-targeted animals developed T-ALL with similar kinetics when crossed to the Lck-cre strain (unpublished data and reference 35). A discrepancy between the two studies exists over the detection of apoptosis in Fbw7$^{-/-}$ LSK cells. However, Matsuoka et al. (44) reported elevated percentages of apoptosis only in HSCs purified from the marrows of severely cytopenic mice 12 wk after deletion. In the studies presented here, the analysis was performed using LSK cells purified from noncytopenic Fbw7$^{-/-}$ mice 3 wk after polyI-polyC deletion. At that time point there was a significant alteration of HSC quiescence and a reduction of LSK (and LT-HSC) absolute cell numbers. In agreement with our findings, Matsuoka et al. (44) failed to detect an increased frequency of apoptosis in HSCs purified from the BM of noncytopenic animals, even at 12 wk after deletion.

There are few other examples of stem cell function or differentiation being regulated by specific E3 ubiquitin ligases (30). Initially, the UBR1/2 E3 ligases were shown to be essential for neurogenesis due to their effects on the differentiation and survival of neural stem cells and progenitors (45). Also, in the neural system, the Mindbomb1 ligase regulates expression of Notch ligands and consequently controls differentiation of neural stem cells (46). Finally, DDB1, an E3 ligase member of the cullin4A complex, is important for the viability, genomic integrity, and maintenance of neural stem cells (47). Information on the role of any of the multiple E3 ligases on HSC function is scarce and indirect. Studies using a panel of chemical proteasome inhibitors have shown that suppression of proteasome function induced cell death in human CD34^{+} hematopoietic progenitors (48). Moreover, primary CD34^{+} leukemic stem cells also enter apoptosis in response to treatment with the MG-132 proteasome inhibitor (49). However, these were crude experiments that cannot address the complexity of regulation of proteasome function in HSCs by the different ubiquitin ligase complexes. Experiments similar to the ones described in this report, which include E3 ligase expression mapping and gene-targeting experiments, are thus essential for the detailed understanding of the importance of ubiquitination in HSC function.

Multiple protein substrates of Fbw7 have been identified. These include the cell cycle regulator cyclin E and transcription factors such as c-Myc and Notch (50) that could directly or indirectly regulate stem cell function. Our protein expression analyses showed no stabilization of Notch1 in the BM of Mx-cre^{+}Fbw7$^{f/f}$ mice. In fact, we were unable to detect any Notch1-IC protein expression at all. This was not due to any technical obstacle, as Notch1 was significantly stabilized and overexpressed in the thymus of these mice. Also, we were unable to detect CD4^{+}8^{+} cells in the Fbw7$^{-/-}$ BM (not depicted), usually a reliable and rapid indicator of aberrant Notch activation (51, 52). However, we cannot exclude that Notch stabilization occurs in a small fraction of LSK cells, and this change in protein expression is below the sensitivity of the experimental method used. Indeed, Matsuoka et al. (44) detected Notch1 overexpression using confocal microscopy of individual Fbw7$^{-/-}$ LSK cells. In agreement with these results, our RT-PCR analysis of Fbw7$^{-/-}$ LSK cells has revealed a persistent overexpression of Hes-1 and Deltex-1, both well-characterized targets of the Notch pathway (Fig. 8 C).

Similar studies excluded a role for stabilization of another Fbw7 substrate, cyclin E. Indeed, we were unable to detect any significant cyclin E stabilization in response to Fbw7 deletion in either total BM cells or purified stem cell and progenitor populations. These findings are consistent with genetic experiments reported by Loeb et al. (51). These investigators have generated "knock-in" mice that express a mutated cyclin E, cyclin E^{T393A}. T393 falls within a canonical Fbw7 recognition degron, and its phosphorylation allows Fbw7 to bind and ubiquitinate cyclin E. Mutated cyclin E was stabilized and expressed at levels several-fold higher in several tissues, including lymphocytes and thymocytes. Despite this overexpression, cyclin E^{T393A}–homozygous mice showed no phenotypic abnormalities in all tissues examined, including the immune system. They also displayed a normal life span with no significant predisposition to autoimmune disease or tumor induction. Together with our protein expression analyses, these elegant genetic studies argue against a role of cyclin E stabilization in HSC function in response to Fbw7 deletion.

On the other hand, our studies suggested that c-Myc could be an attractive target, especially because it was previously shown to be involved in HSC differentiation (11).

Indeed, both total and phosphorylated c-Myc protein was consistently up-regulated in Fbw7$^{-/-}$ BM stem cells and progenitors. These observations were consistent with the confocal microscopy studies reported by Matsuoka et al. (44), strongly suggesting that c-Myc is indeed an important Fbw7 substrate. Putative targets of c-Myc, including p57^{kip2}, E2F2, and Ccnd1, were also up-regulated in Fbw7$^{-/-}$ LSK cells. In agreement with this hypothesis, Wilson et al. (11) have performed experiments in which they have overexpressed c-Myc specifically in LSK cells. Despite proper homing and inhibition of apoptosis, c-Myc–overexpressing HSCs failed to self-renew, a phenotype similar to the one reported here (11). We should add here that although c-Myc appears to represent an important Fbw7 target, it is possible that there are other yet-unidentified Fbw7 substrates that are important for the hematopoietic phenotypes reported here.

Our presented studies identify Fbw7 as a novel essential regulator of HSC quiescence and self-renewal. Initially, deletion of Fbw7, which was normally expressed at high levels in noncycling HSCs, affects the expression of key regulators of cell cycle entry, including the D-type cyclin Ccnd1, the cell cycle inhibitor p57^{kip2}, and the downstream transcriptional effector E2F2. The combined action of these regulators could induce exit from quiescence and cell cycle entry, as the BrdU incorporation experiments convincingly demonstrated that upon Fbw7 deletion >80% of LT-HSCs have entered cell cycle. It is tempting to hypothesize that aberrant cell cycle entry forces Fbw7$^{-/-}$ HSCs to exit the quiescent niche and lose their self-renewing ability. Once more, our expression studies provide mechanistic support to this hypothesis. Fbw7 deletion dramatically suppresses the expression of several genes (*Mpl*, *Pbx3*, *p57*, *Meis1*, *Evi1*, *Eya1/2*, *Angpt*, *Thy1*, and *Ndn*) that define a partial "LT-HSC" transcriptional signature (Table S1 and unpublished data).

The identification of Fbw7 as a key regulator of HSC quiescence and self-renewal may have very significant biological repercussions. Initially, Fbw7 function could be important for self-renewal of cancer stem cells with important implications in the therapeutic targeting of their maintenance. In agreement with this notion, Fbw7 deletion suppresses the expression of several genes involved in hematopoietic transformation (*Ccnd1*, *Evi1*, *Pbx3*, and *Meis1*). It is intriguing to mention here that Fbw7 can also function as a tumor suppressor when deleted in T cells using the Lck-cre^{+}Fbw7$^{f/f}$ model (reference 35 and unpublished data), suggesting that Fbw7 function in oncogenesis could differ between uncommitted stem cells, committed progenitors, and mature lymphocytes. For all these reasons, the identification of regulators of Fbw7 activity, including specific deubiquitinating enzymes or substrate-specific priming kinases, could be valuable for both the development of HSC transplantation protocols and the suppression of transformation.

MATERIALS AND METHODS

Generation of the Fbw7^{flox} mice. An ~11.5-kb region used to generate the targeting vector was subcloned from a positively identified C57B6 BAC clone using homologous recombination. The region was designed such that the short homology arm extends 2.4 kb 5′ to loxP/FTR-flanked NEO cassette. The long homology arm ends on the 3′ side of the loxP/FRT NEO cassette and was ~8-kb long. A single lox P site was inserted upstream of exon 5. The target region was 2.1 kb and included exons 5 and 6. The backbone vector was ~2.1 kb and contained an ampicillin selection cassette. The total size of the targeting construct (including the vector backbone) was ~16 kb. The targeting vector was linearized using NotI and electroporated into 129 Sv/En × C57BL6 hybrid ES cells. After G418 selection, surviving clones were expanded for PCR analysis to identify recombinant ES cell clones. Oligos for ES cell screening and PCR conditions are available upon request. Five correctly targeted ES cell clones were expanded for microinjection into blastocysts. Strong chimeras were identified and crossed to C57BL6 females to verify germline transmission. The F1 generation was PCR screened and crossed to FLP recombinase–expressing mice (Jax mice) to delete the Frt-flanked Neo Cassette. Fbw7$^{flox/Neo-}$ mice were consequently crossed to Mx1-cre and Lck-cre mice.

For our polyI-polyC experiments, we injected 20 μg polyI-polyC per gram of body weight. We initiated injections 2 wk after birth. Mice were injected once every other day for a total of three injections. They were analyzed 1, 2, and 4 wk after injection. All animal experiments were approved by the IACUC of the NYU School of Medicine.

Transplantation assays. For the experiment shown in Fig. 4, we have mixed BM from either CD45.2 Mx-cre^{+}Fbw7$^{wt/wt}$ or CD45.2 Mx-cre^{+}Fbw7$^{f/f}$ mice (2 wk after the end of polyI-polyC treatment) with WT CD45.1 cells. We normalized for absolute numbers of LSK cells in each marrow such that we injected 1,000 LSK cells from each genotype. The cells were injected in lethally (900 rad) irradiated CD45.1 congenic H57BL6 recipients. We analyzed chimerism 5 wk after transplant.

For the experiment shown in Fig. S4, we mixed (50:50) nonpolyI-polyC–injected whole BM cells (CD45.2 Mx-cre^{+}Fbw7$^{wt/wt}$ or CD45.2 Mx-cre^{+}Fbw7$^{f/f}$ with WT CD45.1 cells). After we verified chimerism from both CD45.1/2 donors (using peripheral blood FACS analysis), we began polyI-polyC injections (three). Chimerism was studied 7 wk after the end of the polyI-polyC treatment.

Genotyping and genomic PCR. Mouse tails were clipped at 1–2 wk of age and incubated in tail lysis buffer for 12–24 h at 55°C. 6M NaCl was added, insoluble debris was pelleted, and DNA was precipitated with isopropanol. The resulting DNA pellets were washed with 70% ethanol and dissolved in water for PCR analysis. Genomic DNA from BM and thymocytes was prepared by lysing the cells in a solution containing 0.03% NP-40, 0.03% Tween 20, and 7 μg/ml proteinase K for 30 min at 55°C, followed by 10 min at 100°C. This solution was used directly for PCR. Primers were designed to selectively amplify WT, targeted (Neo+), targeted (Neo−), and CKO Fbw7 alleles as shown in Fig. 2. The sequences are as follows: A F, 5′-GGCTTAGCATATCAGCTATGG; B F, 5′-ATTGATACAAACTGGAGACGAGG; C R, 5′-ATAGTAATCCTCCTGCCTTGGC; and D F, 5′-TGCGAGGCCAGAGGCCACTTGTGTAGC. MxCre and LckCre transgenes were detected using the following primers: Cre F, 5′-GCGGTCTGGCAGTAAAAACTATC; Cre R, 5′-AAGTGACAGCAATGCTGTTTCAC; and LckF, 5′-GGTTTGCCCATCCCAGGTG. All PCRs used a T_m = 58°C for 35 cycles, except for Cre PCRs, which used a T_m = 52°C.

Antibodies and FACS analysis. Antibody staining and FACS analysis was performed as described previously (11). All antibodies were purchased from BD Biosciences or eBioscience. We used the following antibodies: c-kit (2B8), Sca-1 (D7), Mac-1 (M1/70), Gr-1 (RB6-8C5), NK1.1 (PK136), TER-119, CD3 (145-2C11), CD19 (1D3), IL7Rα (A7R34), CD34 (RAM34), FcγII/III (2.4G2), Flk-2/Flt-3 (A2F10.1), CD4 (RM4-5), CD4 (H129.19), CD8 (53–6.7), CD25 (PC61), and CD44 (IM7). BM lineage antibody cocktail includes the following: Mac-1, Gr-1, NK1.1, TER-119, CD3, TCR-β, TCR-γδ, and CD19.

Microarray analysis and quantitative PCR validation. For gene expression profiling of primary HSC and progenitor cell subsets, we pooled hind limb BM cells from three mice. Freshly isolated cells were sorted by surface marker expression, and total RNA was extracted using the RNAEasy kit (QIAGEN). To generate sufficient sample quantities for oligonucleotide gene chip hybridization and quantitative PCR experiments, we used the GeneChip Two-Cycle cDNA Synthesis kit (Affymetrix) for cRNA amplification and labeling. The amplified cRNA was labeled and hybridized to the MOE430 Plus 2 oligonucleotide arrays (Affymetrix) or reverse-transcribed using the First Strand cDNA Synthesis kit (Invitrogen) for quantitative PCR experiments. The Affymetrix gene expression profiling data were normalized using the previously published Robust Multi-array Average algorithm using the GeneSpring 7 software (Agilent Technologies). Messenger RNA expression levels for critical regulators of HSC proliferation and self-renewal were verified by quantitative PCR using the 7900 Real Time PCR system (Applied Biosystems). Primers and probes used were purchased from Applied Biosystems. The relative expression of target genes was calculated using the delta–delta Ct method and normalized to the HPRT mRNA content. Two biological duplicates were used for each quantitative RT-PCR experiment. Each duplicate included a mixture of cells (LSK or MP) sorted from two mice with the same genotype for each experiment. Microarray data were deposited in the GEO database under accession numbers GSE11178, GSM281722, GSM281723, GSM281724, and GSM281725.

RT-PCR. Total RNA was isolated using the RNeasy Plus Mini kit (QIAGEN) and used to synthesize cDNA with the SuperScript First-Strand kit (Invitrogen). Real-time quantitative PCR was performed using iQ SYBR Green Supermix and an iCycler (Bio-Rad Laboratories) using the following primer sequences (T_m = 60°C for all primers): Fbw7 F, 5′-GTGATAGAGCCCCAGTTCCA and Fbw7 R, 5′-CCTCAGCCAAAATTCTCCAG; Deltex1 F, 5′-GAGGTCCACCAGCGTCAG and Deltex1 R, 5′- GCCAGTGCCATTCAAGTTCT; Cul1 F, 5′-GGAAGACCGCAAACTACTGA and Cul1 R, 5′-GTGTCCTTCTCACCATCGAC; and Actin F, 5′-TGGAATCCTGTGGCATCCATGAAAC and Actin R, 5′-TAAAACGCAGCTCCAGTAACAGTCCG. Expression levels for each transcript were normalized to Actin expression. For Fbw7 isoform PCR, cDNA was prepared as described above and amplified (T_m = 55°C, 38 cycles) using each of the following forward primers: Fbw7α F, 5′-GGAGATGGACCAGGAGAGTG; Fbw7β F, 5′-TTGTCAGAGACTGCCAAGCA; and Fbw7γ F, 5′-ATGGCTTGGTTCCTGTTGAT paired with a common reverse primer: Fbw7exon3 R, 5′-GTTGGTGTTGCTGAACATGG. PCR products were separated on 2% agarose gels and visualized with ethidium bromide staining.

BrdU incorporation. Mice received an intraperitoneal injection of 3 mg BrdU (Becton Dickinson), and 1 mg/ml BrdU (Sigma-Aldrich) was added to the drinking water for 42 h. BrdU detection in LSK cells was performed as described previously (52).

Western blotting. Total cell lysates were prepared as described previously (25), separated on 4–15% gradient Tris-HCl gels (Bio-Rad Laboratories), and transferred to nitrocellulose or PVDF. Membranes were probed with the following antibodies: Notch1-IC (Notch1 Val1744; Cell Signaling Technology), pan-Notch1 (C-20; Santa Cruz Biotechnology, Inc.), c-Myc (no. 06-340; Millipore), phospho-c-Myc (T58/S62; Cell Signaling Technology), Cyclin E (M-20; Santa Cruz Biotechnology, Inc.), and Actin (MAB1501R; Millipore).

Methylcellulose assays. LSK cells were sorted from control ($Fbw7^{f/f}$ Mx1-Cre^{-}) or CKO ($Fbw7^{f/f}$Mx1-Cre^{+}) mice 2 wk after polyI:C injection. LSK cells were plated in duplicate (500 LSK/35-mm dish) into cytokine-supplemented methycellulose medium (MethoCult 3434; Stem Cell Technologies), and the number and morphology of colonies were scored 7 d later.

In vitro LSK culture. LSK cells were sorted from 4–8-wk-old C57/B6 mice and plated in 96-well plates (5,000 LSK per well) in OPTI-MEM supplemented with 10% fetal bovine serum, 50 ng/ml Flt3 ligand, 50 ng/ml SCF, 10 ng/ml IL-6, and 10 ng/ml IL-3 (53). Cells were harvested at different time points for cell cycle analysis and quantitative PCR. For cell cycle analysis, cells were fixed and permeabilized according to the manufacturer's instructions (Fix and Perm; Invitrogen) and stained with PE-conjugated anti–Ki-67 (BD Biosciences) or control anti-IgG antibody. Cells were then resuspended in PBS containing 5 μg/ml RNaseA and 2 μg/ml DAPI, and analyzed by flow cytometry.

Statistical analysis. The means of each dataset were analyzed using the Student's *t* test, with a two-tailed distribution and assuming equal sample variance. Data were considered statistically significant when $P < 0.05$. Significant data are noted in the manuscript as follows: *, $P < 0.05$; **, $P < 0.005$.

Online supplemental material. Fig. S1 shows Fbw7 expression in different blood subsets. Fig. S2 shows stabilization of Notch1 in the thymus. Fig. S3 shows the phenotype of Lck-$Cre^{+}Fbw7^{f/f}$ thymi. Fig. S4 demonstrates that the $Fbw7^{-/-}$ phenotype is cell autonomous. Fig. S5 shows that the cell cycle defect is specific to HSC. The online supplemental material is available at http://www.jem.org/cgi/content/full/jem.20080277/DC1.

We would like to thank Steve Yu for help with the generation of the $Fbw7^{flox}$ mice, Peter Lopez for excellent FACS support, and Barry Sleckman for c-Myc protein expression advice and the sharing of reagents.

The Aifantis laboratory is supported by a generous donation by the Helen L. and Martin S. Kimmel Stem Cell Center. This work is supported by the National Institutes of Health (R56AI070310 and RO1CA105129 to I. Aifantis), the American Cancer Society (RSG0806801 to I. Aifantis), the Leukemia and Lymphoma Society (Scholar Award to I. Aifantis), the Chemotherapy Foundation, the G&P Foundation for Cancer Research, and the Edward Mallinkcrodt, Jr. Foundation (to I. Aifantis). S.D. Nimer was supported by NIHRO1 DK52208 and a Leukemia Lymphoma Society SCOR Award. S. Buonamici was supported by an NYU Molecular Oncology and Immunology training grant (T32 CA-09161) and by an American Society of Hematology Scholar Award.

The authors have no conflicting financial interests.

Submitted: 11 February 2008
Accepted: 18 April 2008

REFERENCES

1. Passegue, E., and A.J. Wagers. 2006. Regulating quiescence: new insights into hematopoietic stem cell biology. *Dev. Cell.* 10:415–417.
2. Aguila, H.L., K. Akashi, J. Domen, K.L. Gandy, E. Lagasse, R.E. Mebius, S.J. Morrison, J. Shizuru, S. Strober, N. Uchida, et al. 1997. From stem cells to lymphocytes: biology and transplantation. *Immunol. Rev.* 157:13–40.
3. Adams, G.B., and D.T. Scadden. 2006. The hematopoietic stem cell in its place. *Nat. Immunol.* 7:333–337.
4. Yin, T., and L. Li. 2006. The stem cell niches in bone. *J. Clin. Invest.* 116:1195–1201.
5. Trowbridge, J.J., M.P. Scott, and M. Bhatia. 2006. Hedgehog modulates cell cycle regulators in stem cells to control hematopoietic regeneration. *Proc. Natl. Acad. Sci. USA.* 103:14134–14139.
6. Trowbridge, J.J., A. Xenocostas, R.T. Moon, and M. Bhatia. 2006. Glycogen synthase kinase-3 is an in vivo regulator of hematopoietic stem cell repopulation. *Nat. Med.* 12:89–98.
7. Duncan, A.W., F.M. Rattis, L.N. DiMascio, K.L. Congdon, G. Pazianos, C. Zhao, K. Yoon, J.M. Cook, K. Willert, N. Gaiano, and T. Reya. 2005. Integration of Notch and Wnt signaling in hematopoietic stem cell maintenance. *Nat. Immunol.* 6:314–322.
8. Blank, U., G. Karlsson, and S. Karlsson. 2008. Signaling pathways governing stem-cell fate. *Blood.* 111:492–503.
9. Karlsson, G., U. Blank, J.L. Moody, M. Ehinger, S. Singbrant, C.X. Deng, and S. Karlsson. 2007. Smad4 is critical for self-renewal of hematopoietic stem cells. *J. Exp. Med.* 204:467–474.

10. Kozar, K., M.A. Ciemerych, V.I. Rebel, H. Shigematsu, A. Zagozdzon, E. Sicinska, Y. Geng, Q. Yu, S. Bhattacharya, R.T. Bronson, et al. 2004. Mouse development and cell proliferation in the absence of D-cyclins. *Cell*. 118:477–491.
11. Wilson, A., M.J. Murphy, T. Oskarsson, K. Kaloulis, M.D. Bettess, G.M. Oser, A.C. Pasche, C. Knabenhans, H.R. Macdonald, and A. Trumpp. 2004. c-Myc controls the balance between hematopoietic stem cell self-renewal and differentiation. *Genes Dev*. 18:2747–2763.
12. Baena, E., M. Ortiz, A.C. Martinez, and I.M. de Alboran. 2007. c-Myc is essential for hematopoietic stem cell differentiation and regulates Lin(-)Sca-1(+)c-Kit(-) cell generation through p21. *Exp. Hematol*. 35:1333–1343.
13. Yang, L., L. Wang, H. Geiger, J.A. Cancelas, J. Mo, and Y. Zheng. 2007. Rho GTPase Cdc42 coordinates hematopoietic stem cell quiescence and niche interaction in the bone marrow. *Proc. Natl. Acad. Sci. USA*. 104:5091–5096.
14. Radtke, F., A. Wilson, G. Stark, M. Bauer, J. van Meerwijk, H.R. MacDonald, and M. Aguet. 1999. Deficient T cell fate specification in mice with an induced inactivation of Notch1. *Immunity*. 10:547–558.
15. Zuniga-Pflucker, J.C. 2004. T-cell development made simple. *Nat. Rev. Immunol*. 4:67–72.
16. Stier, S., T. Cheng, D. Dombkowski, N. Carlesso, and D.T. Scadden. 2002. Notch1 activation increases hematopoietic stem cell self-renewal in vivo and favors lymphoid over myeloid lineage outcome. *Blood*. 99:2369–2378.
17. Han, H., K. Tanigaki, N. Yamamoto, K. Kuroda, M. Yoshimoto, T. Nakahata, K. Ikuta, and T. Honjo. 2002. Inducible gene knockout of transcription factor recombination signal binding protein-J reveals its essential role in T versus B lineage decision. *Int. Immunol*. 14:637–645.
18. Mancini, S.J., N. Mantei, A. Dumortier, U. Suter, H.R. Macdonald, and F. Radtke. 2005. Jagged1-dependent Notch signaling is dispensable for hematopoietic stem cell self-renewal and differentiation. *Blood*. 105:2340–2342.
19. Wilson, A., D.L. Ardiet, C. Saner, N. Vilain, F. Beermann, M. Aguet, H.R. Macdonald, and O. Zilian. 2007. Normal hemopoiesis and lymphopoiesis in the combined absence of numb and numblike. *J. Immunol*. 178:6746–6751.
20. Nakayama, K.I., and K. Nakayama. 2006. Ubiquitin ligases: cell-cycle control and cancer. *Nat. Rev. Cancer*. 6:369–381.
21. Minella, A.C., and B.E. Clurman. 2005. Mechanisms of tumor suppression by the SCF(Fbw7). *Cell Cycle*. 4:1356–1359.
22. Ye, X., G. Nalepa, M. Welcker, B.M. Kessler, E. Spooner, J. Qin, S.J. Elledge, B.E. Clurman, and J.W. Harper. 2004. Recognition of phosphodegron motifs in human cyclin E by the SCF(Fbw7) ubiquitin ligase. *J. Biol. Chem*. 279:50110–50119.
23. Orlicky, S., X. Tang, A. Willems, M. Tyers, and F. Sicheri. 2003. Structural basis for phosphodependent substrate selection and orientation by the SCFCdc4 ubiquitin ligase. *Cell*. 112:243–256.
24. Koepp, D.M., L.K. Schaefer, X. Ye, K. Keyomarsi, C. Chu, J.W. Harper, and S.J. Elledge. 2001. Phosphorylation-dependent ubiquitination of cyclin E by the SCFFbw7 ubiquitin ligase. *Science*. 294:173–177.
25. Thompson, B.J., S. Buonamici, M.L. Sulis, T. Palomero, T. Vilimas, G. Basso, A. Ferrando, and I. Aifantis. 2007. The SCFFBW7 ubiquitin ligase complex as a tumor suppressor in T cell leukemia. *J. Exp. Med*. 204:1825–1835.
26. O'Neil, J., J. Grim, P. Strack, S. Rao, D. Tibbitts, C. Winter, J. Hardwick, M. Welcker, J.P. Meijerink, R. Pieters, et al. 2007. FBW7 mutations in leukemic cells mediate NOTCH pathway activation and resistance to γ-secretase inhibitors. *J. Exp. Med*. 204:1813–1824.
27. Malyukova, A., T. Dohda, N. von der Lehr, S. Akhondi, M. Corcoran, M. Heyman, C. Spruck, D. Grander, U. Lendahl, and O. Sangfelt. 2007. The tumor suppressor gene hCDC4 is frequently mutated in human T-cell acute lymphoblastic leukemia with functional consequences for Notch signaling. *Cancer Res*. 67:5611–5616.
28. Akhoondi, S., D. Sun, N. von der Lehr, S. Apostolidou, K. Klotz, A. Maljukova, D. Cepeda, H. Fiegl, D. Dofou, C. Marth, et al. 2007. FBXW7/hCDC4 is a general tumor suppressor in human cancer. *Cancer Res*. 67:9006–9012.
29. Maser, R.S., B. Choudhury, P.J. Campbell, B. Feng, K.K. Wong, A. Protopopov, J. O'Neil, A. Gutierrez, E. Ivanova, I. Perna, et al. 2007. Chromosomally unstable mouse tumours have genomic alterations similar to diverse human cancers. *Nature*. 447:966–971.
30. Naujokat, C., and T. Saric. 2007. Concise review: role and function of the ubiquitin-proteasome system in mammalian stem and progenitor cells. *Stem Cells*. 25:2408–2418.
31. Tsunematsu, R., K. Nakayama, Y. Oike, M. Nishiyama, N. Ishida, S. Hatakeyama, Y. Bessho, R. Kageyama, T. Suda, and K.I. Nakayama. 2004. Mouse Fbw7/Sel-10/Cdc4 is required for notch degradation during vascular development. *J. Biol. Chem*. 279:9417–9423.
32. Tetzlaff, M.T., W. Yu, M. Li, P. Zhang, M. Finegold, K. Mahon, J.W. Harper, R.J. Schwartz, and S.J. Elledge. 2004. Defective cardiovascular development and elevated cyclin E and Notch proteins in mice lacking the Fbw7 F-box protein. *Proc. Natl. Acad. Sci. USA*. 101:3338–3345.
33. Kuhn, R., F. Schwenk, M. Aguet, and K. Rajewsky. 1995. Inducible gene targeting in mice. *Science*. 269:1427–1429.
34. El Andaloussi, A., S. Graves, F. Meng, M. Mandal, M. Mashayekhi, and I. Aifantis. 2006. Hedgehog signaling controls thymocyte progenitor homeostasis and differentiation in the thymus. *Nat. Immunol*. 7:418–426.
35. Onoyama, I., R. Tsunematsu, A. Matsumoto, T. Kimura, I.M. de Alboran, K. Nakayama, and K.I. Nakayama. 2007. Conditional inactivation of Fbxw7 impairs cell-cycle exit during T cell differentiation and results in lymphomatogenesis. *J. Exp. Med*. 204:2875–2888.
36. Passegue, E., A.J. Wagers, S. Giuriato, W.C. Anderson, and I.L. Weissman. 2005. Global analysis of proliferation and cell cycle gene expression in the regulation of hematopoietic stem and progenitor cell fates. *J. Exp. Med*. 202:1599–1611.
37. Terskikh, A.V., T. Miyamoto, C. Chang, L. Diatchenko, and I.L. Weissman. 2003. Gene expression analysis of purified hematopoietic stem cells and committed progenitors. *Blood*. 102:94–101.
38. Jankovic, V., A. Ciarrocchi, P. Boccuni, T. DeBlasio, R. Benezra, and S.D. Nimer. 2007. Id1 restrains myeloid commitment, maintaining the self-renewal capacity of hematopoietic stem cells. *Proc. Natl. Acad. Sci. USA*. 104:1260–1265.
39. Forsberg, E.C., S.S. Prohaska, S. Katzman, G.C. Heffner, J.M. Stuart, and I.L. Weissman. 2005. Differential expression of novel potential regulators in hematopoietic stem cells. *PLoS Genet*. 1:e28.
40. Mansson, R., A. Hultquist, S. Luc, L. Yang, K. Anderson, S. Kharazi, S. Al-Hashmi, K. Liuba, L. Thoren, J. Adolfsson, et al. 2007. Molecular evidence for hierarchical transcriptional lineage priming in fetal and adult stem cells and multipotent progenitors. *Immunity*. 26:407–419.
41. Dauphinot, L., C. De Oliveira, T. Melot, N. Sevenet, V. Thomas, B.E. Weissman, and O. Delattre. 2001. Analysis of the expression of cell cycle regulators in Ewing cell lines: EWS-FLI-1 modulates p57KIP2 and c-Myc expression. *Oncogene*. 20:3258–3265.
42. Daksis, J.I., R.Y. Lu, L.M. Facchini, W.W. Marhin, and L.J. Penn. 1994. Myc induces cyclin D1 expression in the absence of de novo protein synthesis and links mitogen-stimulated signal transduction to the cell cycle. *Oncogene*. 9:3635–3645.
43. Leone, G., R. Sears, E. Huang, R. Rempel, F. Nuckolls, C.H. Park, P. Giangrande, L. Wu, H.I. Saavedra, S.J. Field, et al. 2001. Myc requires distinct E2F activities to induce S phase and apoptosis. *Mol. Cell*. 8:105–113.
44. Matsuoka, S., Y. Oike, I. Onoyama, A. Iwama, F. Arai, K. Takubo, Y. Mashimo, H. Oguro, E. Nitta, K. Ito, et al. 2008. Fbxw7 acts as a critical fail-safe against premature loss of hematopoietic stem cells and development of T-ALL. *Genes Dev*. 22:986–991.
45. An, J.Y., J.W. Seo, T. Tasaki, M.J. Lee, A. Varshavsky, and Y.T. Kwon. 2006. Impaired neurogenesis and cardiovascular development in mice lacking the E3 ubiquitin ligases UBR1 and UBR2 of the N-end rule pathway. *Proc. Natl. Acad. Sci. USA*. 103:6212–6217.
46. Barsi, J.C., R. Rajendra, J.I. Wu, and K. Artzt. 2005. Mind bomb1 is a ubiquitin ligase essential for mouse embryonic development and Notch signaling. *Mech. Dev*. 122:1106–1117.
47. Cang, Y., J. Zhang, S.A. Nicholas, A.L. Kim, P. Zhou, and S.P. Goff. 2007. DDB1 is essential for genomic stability in developing epidermis. *Proc. Natl. Acad. Sci. USA*. 104:2733–2737.

48. Daino, H., H. Shibayama, T. Machii, and T. Kitani. 1996. Extracellular ubiquitin regulates the growth of human hematopoietic cells. *Biochem. Biophys. Res. Commun.* 223:226–228.
49. Naujokat, C., O. Sezer, H. Zinke, A. Leclere, S. Hauptmann, and K. Possinger. 2000. Proteasome inhibitors induced caspase-dependent apoptosis and accumulation of p21WAF1/Cip1 in human immature leukemic cells. *Eur. J. Haematol.* 65:221–236.
50. Welcker, M., and B.E. Clurman. 2008. FBW7 ubiquitin ligase: a tumour suppressor at the crossroads of cell division, growth and differentiation. *Nat. Rev. Cancer.* 8:83–93.
51. Loeb, K.R., H. Kostner, E. Firpo, T. Norwood, D.K. Tsuchiya, B.E. Clurman, and J.M. Roberts. 2005. A mouse model for cyclin E-dependent genetic instability and tumorigenesis. *Cancer Cell.* 8:35–47.
52. Lacorazza, H.D., T. Yamada, Y. Liu, Y. Miyata, M. Sivina, J. Nunes, and S.D. Nimer. 2006. The transcription factor MEF/ELF4 regulates the quiescence of primitive hematopoietic cells. *Cancer Cell.* 9:175–187.
53. Ciarrocchi, A., V. Jankovic, Y. Shaked, D.J. Nolan, V. Mittal, R.S. Kerbel, S.D. Nimer, and R. Benezra. 2007. Id1 restrains p21 expression to control endothelial progenitor cell formation. *PLoS ONE.* 2:e1338.